PHYSICAL REVIEW B VOLUME 50, NUMBER 10 1 SEPTEMBER 1994-II

Electronic phase separation: Extended mean-field calculations for CuO_2 layers in high-T_c superconductors

D. Klemm and M. Letz
Institut für Theoretische Physik der Universität Stuttgart, Pfaffenwaldring 57, D-70550 Stuttgart, Germany

E. Sigmund
Institut für Theoretische Physik der Universität Stuttgart, Pfaffenwaldring 57, D-70550 Stuttgart, Germany
and Technische Universität Cottbus, Lehrstuhl für Theoretische Physik, Karl-Marx-Strasse 17, D-03044 Cottbus, Germany

G. S. Zavt
Institut für Theoretische Physik der Universität Stuttgart, Pfaffenwaldring 57, D-70550 Stuttgart, Germany
and Estonian Academy of Sciences, Institute of Physics, Riia 142, EE 2400 Tartu, Estonia

(Received 29 December 1993)

We examine the stability of spin-polarized cluster states (ferrons) which appear by hole doping of the antiferromagnetically ordered CuO_2 planes in the high-T_c cuprates. The influence of additional holes is calculated within a self-consistent mean-field-type approximation. The variation procedure for the spin polarization is extended over up to five CuO_2 plaquettes. Different correlation terms (U_{pd}, U_p) affecting the cluster stability are discussed. For all cases the cluster binding energy and the polarization of the Cu spins are calculated. In addition the interaction between different clusters is discussed.

I. INTRODUCTION

In the parent materials for the high-T_c cuprates [e.g., $La_{2-x}(Sr,Ba)_xCuO_4$ or $YBaCuO_{6+y}$] the doping $(x,y>0)$ evokes a transition from an antiferromagnetic insulator to a conducting and below T_c superconducting state. Doping in this system means that the geometrical structure of the CuO_2 layers remains unperturbed, while holes are introduced into the planes.

Different theoretical works show that an excess hole slightly perturbs the electronic structure in its vicinity by forming a spin-polarized cluster. Such states, often also denoted as magnetic polarons or ferrons, are discussed not only in high-T_c materials. For a review see, e.g., Ref. 1. In the context of cuprate superconductors there have been several attempts to explain pairing mechanisms by magnetic polarons.[2-4] In contrast to that in our calculations the interaction between the clusters turns out to be extremely small. Furthermore most authors that regard magnetic polarons do not consider a turn of polarization in an original antiferromagnetically ordered lattice, but instead get a spin bag.[3,5,6] Ferrons with a turned spin were already derived with the *t-J* model.[7,8]

At higher doping concentrations the clusters start to build up a microscopic percolation network.[9] In this way a phase transition from an antiferromagnetic insulator to a conducting state is established.

This scenario is confirmed by many experiments that show either the existence of spin-polarized clusters[10,11] or prove a phase transition of such a percolative type.[12] In our calculations we emphasize the effect of a single hole. We start from the unperturbed configuration, whose antiferromagnetic order is determined self-consistently after doubling the elementary cell.

An additional hole leads to the variation of the spin polarization. The new spin expectation values are calculated self-consistently both for one and five CuO_2 plaquettes. For the usual parameters for the high-T_c cuprates the resulting state turns out to be a spin-polarized cluster. The effect of higher doping is discussed by introducing several holes into the cluster. A Coulomb repulsion on oxygen sites (U_p) and an intersite Coulomb repulsion between copper and oxygen electrons (U_{pd}) is also taken into account. By calculating the binding energy we discuss the stability of the clusters. Furthermore we regard the interaction between different clusters which turns out to be very weak.

II. SELF-CONSISTENT APPROACH

We start from the three-band Hubbard Hamiltonian in the electron picture

$$H=\epsilon_d\sum_{m\sigma}n^d_{m\sigma}+\epsilon_p\sum_{m'\sigma}n^p_{m'\sigma}+T\sum_{(mm')\sigma}(d^\dagger_{m\sigma}p_{m'\sigma}+\text{H.c.})+U\sum_m n^d_{m\uparrow}n^d_{m\downarrow}\ , \tag{1}$$

where ϵ_d and ϵ_p are on-site energies at copper and oxygen sites, respectively. T is the transfer integral between oxygen and copper sites and the Hubbard energy U describes the Coulomb repulsion between two electrons at the same copper site. The parameters are usually assumed to be of order of $T\approx1$ eV, $U\approx8$ eV, and $\epsilon=\epsilon_p-\epsilon_d\approx3$ eV.[13,14] $d\,(d^\dagger)$ and $p\,(p^\dagger)$ denote electronic annihilation (creation) operators on the $d_{x^2-y^2}$ copper and the $p_{x,y}$ oxygen orbitals. $n^d=d^\dagger d$ and $n^p=p^\dagger p$ are occupation number operators. (mm') represents the summation over nearest neighbors only.

The structural elementary cell consists of one CuO_2 unit. In the undoped case the oxygen sites are mainly doubly occupied, while there is one electron on each copper site. The spins of the copper electrons are arranged antiferromagnetically.

In order to handle the strong correlations described by the Hubbard term the following mean-field approximation which is known to be reasonable for larger U/T is used:

$$\begin{aligned} U n_{i,\sigma}^{d} n_{i,-\sigma}^{d} \approx\ & U n_{i,\sigma}^{d} \langle n_{i,-\sigma}^{d} \rangle + U \langle n_{i,\sigma}^{d} \rangle n_{i,-\sigma}^{d} \\ & - U \langle n_{i,\sigma}^{d} \rangle \langle n_{i,-\sigma}^{d} \rangle . \end{aligned} \tag{2}$$

There also exists a different approach in which the correlation terms are treated with a slave-boson technique.[15] This additionally leads to a renormalization of the transfer integral. The results do not differ strongly from ours, except that all polarizations become slightly smaller. However, in such a slave-boson approach further correlations and an enlargement of the variation procedure are difficult to introduce. Therefore we restrict ourselves to a Hartree-Fock approximation. Then the Hamiltonian reads

$$H = \sum_{\sigma} H_{\mathrm{MF}}^{\sigma} - U \sum_{i} \langle n_{i\sigma}^{d} \rangle \langle n_{i-\sigma}^{d} \rangle \tag{3}$$

with

$$\begin{aligned} H_{\mathrm{MF}}^{\sigma} = & \sum_{m} (\epsilon_d + U \langle n_{m-\sigma}^{d} \rangle) n_{m\sigma}^{d} + \epsilon_p \sum_{m'} n_{m'\sigma}^{p} \\ & + T \sum_{(mm')} (d_{m\sigma}^{\dagger} p_{m'\sigma} + \mathrm{H.c.}) . \end{aligned} \tag{4}$$

A. Unperturbed antiferromagnet

As we want to describe the antiferromagnetic order, we double the elementary cell. Due to the renormalization the two copper on-site energies in the magnetic elementary cell are given by

$$\begin{aligned} \epsilon_{1\sigma} &= \epsilon_d + U \langle n_{1-\sigma}^{d} \rangle , \\ \epsilon_{2\sigma} &= \epsilon_d + U \langle n_{2-\sigma}^{d} \rangle . \end{aligned} \tag{5}$$

From the symmetry of the antiferromagnetic state it follows immediately that

$$\langle n_{1\sigma}^{d} \rangle = \langle n_{2-\sigma}^{d} \rangle . \tag{6}$$

Therefore we can use the notation $\langle n_{\sigma}^{d} \rangle$ and regard these quantities as being modulated with twice the lattice period.

Let us consider the Hamiltonian H_{MF}^{σ} for a fixed spin direction, say $\sigma = \uparrow$. In k space it reads

$$\langle k \uparrow | H_{\mathrm{MF}}^{\uparrow} | k \uparrow \rangle = \begin{bmatrix} \epsilon_1 & 0 & -2Ta_x & 2Ta_y & 2Ta_x^* & -2Ta_y^* \\ 0 & \epsilon_2 & 2Ta_x^* & 2Ta_y^* & -2Ta_x & 2Ta_y \\ -2Ta_x^* & 2Ta_x & \epsilon_p & 0 & 0 & 0 \\ 2Ta_y^* & -2Ta_y & 0 & \epsilon_p & 0 & 0 \\ 2Ta_x & -2Ta_x^* & 0 & 0 & \epsilon_p & 0 \\ -2Ta_y & 2Ta_y^* & 0 & 0 & 0 & \epsilon_p \end{bmatrix} \tag{7}$$

with the abbreviation

$$a_{x,y} = \tfrac{1}{2} e^{i k_{x,y} (a/2)} \tag{8}$$

and

$$\epsilon_{1,2} = \epsilon_d + U \langle n_{\downarrow,\uparrow}^{d} \rangle . \tag{9}$$

Symmetric linear combinations of the oxygen states lead to the decoupling of two dispersionless bands of oxygen type. Four bands remain: An upper and lower Hubbard band of mainly copper character and two broader bands of mainly oxygen type between them. In the undoped case the lowest three bands are occupied with electrons (see Fig. 1). Now we can calculate local Green's functions according to

$$G_{ij}^{0\sigma} = [(E - H_{\mathrm{MF}}^{\sigma})^{-1}]_{ij} , \tag{10}$$

which turn out to be linear combinations of complete elliptical integrals. Introducing

$$\begin{aligned} D_i(E) &= (E - \epsilon_i)(E - \epsilon_p) - 4T^2 \quad (i = 1,2) , \\ D(E) &= D_1(E) D_2(E) , \\ \eta^2 &= \frac{D(E)}{16 T^4} , \end{aligned} \tag{11}$$

we obtain, e.g.,

(i) for $\eta^2 > 1$

$$\begin{aligned} G_{00}^{0\uparrow} &= 2 \frac{E - \epsilon_p}{\pi D_1} \mathbf{K} \left[\frac{1}{\eta} \right] , \\ G_{00}^{0\downarrow} &= 2 \frac{E - \epsilon_p}{\pi D_2} \mathbf{K} \left[\frac{1}{\eta} \right] , \end{aligned} \tag{12}$$

(ii) for $0 < \eta^2 < 1$

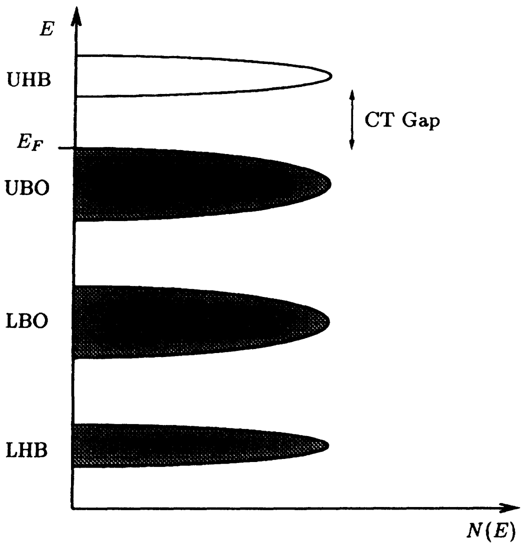

FIG. 1. Bandstructure of the unperturbed antiferromagnet. LHB = lower Hubbard band, UHB = upper Hubbard band, LBO = lower band oxygen, UBO = upper band oxygen.

$$G_{00}^{0\uparrow}=\frac{E-\epsilon_p}{2\pi T^2}\sqrt{D_2/D_1}[\mathbf{K}(\eta)+i\mathbf{K}(\sqrt{1-\eta^2})]\ ,$$
$$G_{00}^{0\downarrow}=\frac{E-\epsilon_p}{2\pi T^2}\sqrt{D_1/D_2}[\mathbf{K}(\eta)+i\mathbf{K}(\sqrt{1-\eta^2})]\ , \tag{13}$$

(iii) for $\eta^2<0$

$$G_{00}^{0\uparrow}=2\frac{E-\epsilon_p}{\pi D_1}\frac{1}{\sqrt{1-1/\eta^2}}\mathbf{K}\left[\frac{1}{\sqrt{1-\eta^2}}\right]\ ,$$
$$G_{00}^{0\downarrow}=2\frac{E-\epsilon_p}{\pi D_2}\frac{1}{\sqrt{1-1/\eta^2}}\mathbf{K}\left[\frac{1}{\sqrt{1-\eta^2}}\right]\ . \tag{14}$$

Here the lower indices of the unperturbed Green's functions $G^{0\sigma}$ denote the lattice sites. $\langle n_{i\sigma}^{d}\rangle$ are determined self-consistently and we get the lowest energy for the antiferromagnetic state as compared with the metallic state. This is in agreement with the results of Refs. 16 and 17.

B. Self-consistent variation at one copper site

Under doping there is the possibility that an electron is taken away from the third band and the ideal antiferromagnetic order remains unchanged. However, due to the nonlinear nature of the mean-field equations one can expect a spontaneous symmetry breaking leading to the creation of localized excitations. We have found that the second scenario leads to a lower ground-state energy in our domain of parameters. It is assumed that the copper spin at site $m=0$ can spontaneously fluctuate, changing the spin densities from $\langle n_{\sigma}^{d}\rangle$ to $\langle n_{\sigma}^{d'}\rangle$. These new values are determined self-consistently. The perturbed Green's function is obtained from the Dyson equation

$$(1-\mathbf{G}^{0\sigma}\mathbf{V}^{\sigma})\mathbf{G}^{\sigma}=\mathbf{G}^{0\sigma}\ . \tag{15}$$

With the perturbation

$$V_{ij}^{\sigma}=U(\langle n_{-\sigma}^{d'}\rangle-\langle n_{-\sigma}^{d}\rangle)\delta_{i0}\delta_{j0} \tag{16}$$

we get

$$G_{00}^{\sigma}=\frac{G_{00}^{0\sigma}}{1-G_{00}^{0\sigma}U(\langle n_{-\sigma}^{d'}\rangle-\langle n_{-\sigma}^{d}\rangle)}\ . \tag{17}$$

The energies of the localized excitations are given by

$$1-G_{00}^{0\sigma}U(\langle n_{-\sigma}^{d'}\rangle-\langle n_{-\sigma}^{d}\rangle)=0\ . \tag{18}$$

The equations for the occupation numbers $\langle n_{\sigma}^{d'}\rangle$ have to be solved self-consistently:

$$\langle n_{\sigma}^{d'}\rangle=\frac{1}{\pi}\int_{-\infty}^{E_F}\mathrm{Im}G_{00}^{\sigma}(\langle n_{-\sigma}^{d'}\rangle,E)dE\ . \tag{19}$$

One localized state splits off from the upper oxygen band into the charge-transfer gap. From this state the electron is removed. Therefore the Fermi energy (E_F) lies between the upper band edge and the localized state (see Fig. 2).

The energy change ΔE due to the perturbation (16) of the Hamiltonian (3) is given by

$$\Delta E=\Delta E^{\mathrm{loc}}+\Delta E^{\mathrm{int}}\ , \tag{20}$$

where ΔE^{loc} arises from the formation of localized levels and reads [$\Delta N_{\sigma}(E)$ is the change of the density of states]

$$\begin{aligned}\Delta E^{\mathrm{loc}}&=\sum_{\sigma}\int_{-\infty}^{E_F}E\Delta N_{\sigma}(E)dE\\&=\frac{1}{\pi}\sum_{\sigma}\int_{-\infty}^{E_F}E\frac{d}{dE}\,\mathrm{Im}[\ln\det(1-\mathbf{G}^{0\sigma}\mathbf{V}^{\sigma})]dE\\&=-\frac{1}{\pi}\sum_{\sigma}\int_{-\infty}^{E_F}\arctan\frac{\mathrm{Im}\det(1-\mathbf{G}^{0\sigma}\mathbf{V}^{\sigma})}{\mathrm{Re}\det(1-\mathbf{G}^{0\sigma}V^{\sigma})}dE\\&\quad+\sum_{i}E_i^L\ .\end{aligned} \tag{21}$$

Here E_i^L signify the energies of the occupied localized states measured from the band edges. ΔE^{int} is essentially

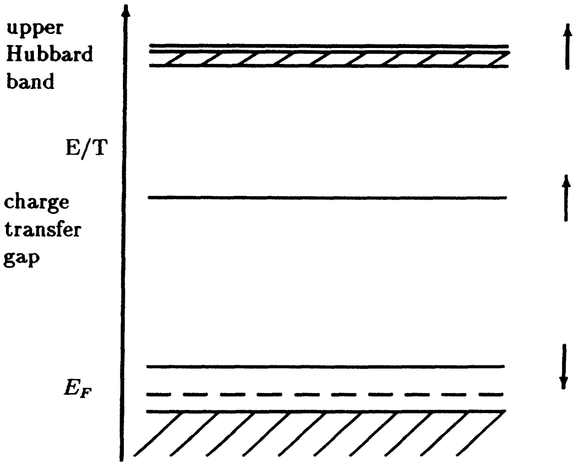

FIG. 2. The situation in the charge-transfer gap for $\epsilon=3$: Two localized states split up, one from the upper Hubbard band and one from the next oxygen band.

the change of the magnetic energy

$$\Delta E^{\text{int}} = U(\langle n_\uparrow^d \rangle \langle n_\downarrow^d \rangle - \langle n_\uparrow^{d'} \rangle \langle n_\downarrow^{d'} \rangle) \ . \tag{22}$$

We report here some results of the calculation for one site regarded self-consistently (see Table I). As one can see the spin at the central copper site is nearly totally turned. Its expectation value changed from 0.116 to 0.79 for spin up and from 0.998 to 0.17 for spin down as a result of this self-consistent calculation with $\epsilon/T=3$ and $U/T=8$. Therefore a cluster of five mainly parallel copper spins is described (see Fig. 3).

Although the perturbation is localized only at one site the spin densities on other Cu sites are also changed. If one added the contribution of the four next neighbors not taken into account self-consistently to the binding energy, it would have the same order of magnitude as the binding energy itself. Thus one has to consider also the four surrounding CuO_2 plaquettes self-consistently.

C. Self-consistent variation at five copper sites

Now we have to solve the Dyson equation for a five-dimensional problem.

$$(1-\mathbf{G}^{0\sigma}\mathbf{V}^{\sigma})\mathbf{G}^{\sigma} = \mathbf{G}^{0\sigma} \tag{23}$$

with

$$\mathbf{V}^{\sigma} = \begin{bmatrix} U\Delta n_\sigma^c & & & & \\ & U\Delta n_\sigma^n & & & \\ & & U\Delta n_\sigma^n & & \\ & & & U\Delta n_\sigma^n & \\ & & & & U\Delta n_\sigma^n \end{bmatrix} ;$$

$$\mathbf{G}^{0\sigma} = \begin{bmatrix} G_{00}^{\sigma} & G_{10} & G_{10} & G_{10} & G_{10} \\ G_{10} & G_{00}^{-\sigma} & G_{20}^{-\sigma} & G_{11}^{-\sigma} & G_{11}^{-\sigma} \\ G_{10} & G_{20}^{-\sigma} & G_{00}^{-\sigma} & G_{11}^{-\sigma} & G_{11}^{-\sigma} \\ G_{10} & G_{11}^{-\sigma} & G_{11}^{-\sigma} & G_{00}^{-\sigma} & G_{20}^{-\sigma} \\ G_{10} & G_{11}^{-\sigma} & G_{11}^{-\sigma} & G_{20}^{-\sigma} & G_{00}^{-\sigma} \end{bmatrix} , \tag{24}$$

TABLE I. Results from a calculation where one copper site was regarded self-consistently and the copper spin on this site was turned. The occupation numbers of the unperturbed AF $\langle n_\uparrow^d \rangle, \langle n_\downarrow^d \rangle$, the values for the perturbed site $\langle n_\uparrow^{d'} \rangle, \langle n_\downarrow^{d'} \rangle$, and the binding energy $-\Delta E/T$ are given. This was done for a Hubbard repulsion $U/T=8$ and for two different values of $\epsilon/T=3$ and 5.

U	ϵ	N	$\langle n_\uparrow^d \rangle$	$\langle n_\downarrow^d \rangle$	$n_\uparrow^{d'} \rangle$	$\langle n_\downarrow^{d'} \rangle$	$-\Delta E$
8	5	1	0.217	0.996	0.84	0.29	0.18
8	3	1	0.116	0.998	0.79	0.17	0.31

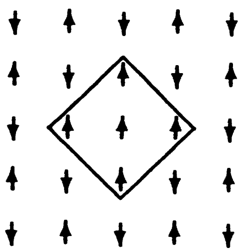

FIG. 3. The situation in the surrounding of an access hole is drawn. The arrows indicate the main direction of the copper spins only as it turns out self-consistently.

where $\Delta n_\sigma^c = \langle n_{-\sigma}^{d'} \rangle^c - \langle n_{-\sigma}^{d} \rangle^c$ is the change in the occupation number of the central copper site, while Δn_σ^n is the one of the four next-nearest neighbors. The symmetry of the problem allows us to transform this equation into three independent and two coupled linear equations

$$\mathbf{T}(1-\mathbf{G}^0\mathbf{V})\mathbf{T}^{-1}\mathbf{T}\mathbf{G} = \mathbf{T}\mathbf{G}^0 \tag{25}$$

with

$$\mathbf{T} = \begin{bmatrix} 1 & & & & \\ & \frac{1}{2} & \frac{1}{2} & \frac{1}{2} & \frac{1}{2} \\ & -\frac{1}{2} & -\frac{1}{2} & \frac{1}{2} & \frac{1}{2} \\ & -\frac{1}{2} & \frac{1}{2} & -\frac{1}{2} & \frac{1}{2} \\ & -\frac{1}{2} & \frac{1}{2} & \frac{1}{2} & -\frac{1}{2} \end{bmatrix} , \tag{26}$$

while $\mathbf{T}(1-\mathbf{G}^0\mathbf{V})\mathbf{T}^{-1}$ has the form

$$\mathbf{T}(1-\mathbf{G}^0\mathbf{V})\mathbf{T}^{-1} = \begin{bmatrix} a_1 & a_2 & & & \\ a_3 & a_4 & & & \\ & & u & & \\ & & & u & \\ & & & & v \end{bmatrix} . \tag{27}$$

The two identical diagonal elements u belong to localized states of the same symmetry given as the zeros of $\det(1-\mathbf{G}^0\mathbf{V})$. They are shown in Fig. 4. We end up with a system of self-consistent equations

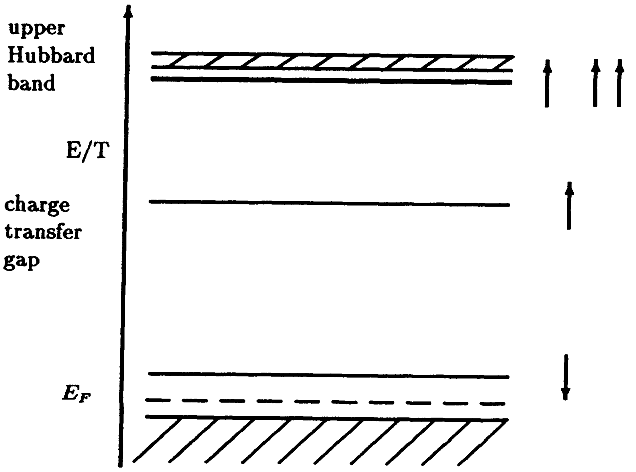

FIG. 4. The situation in the charge-transfer gap for $\epsilon=3$: The localized energy level near the upper Hubbard band is now split into three states, while the other two levels do not shift much compared with Fig. 2.

$$\langle n_\sigma^{d'} \rangle^{c/n} = \frac{1}{\pi} \int_{-\infty}^{E_F} \mathrm{Im}(G_{jj}^{ii}(E, \langle n_{-\sigma}^{d'} \rangle^c, \langle n_{-\sigma}^{d'} \rangle^n, \ldots))dE \ . \tag{28}$$

ΔE is calculated in the same way as in the previous chapter [see Eqs. (20)–(22)] with the exception of ΔE^{int} that now reads

$$\Delta E^{\mathrm{int}} = U(5\langle n_\uparrow^d \rangle \langle n_\downarrow^d \rangle - \langle n_\uparrow^{d'} \rangle^c \langle n_\downarrow^{d'} \rangle^c - 4\langle n_\uparrow^{d'} \rangle^n \langle n_\downarrow^{d'} \rangle^n) \ . \tag{29}$$

Compared with Sec. II B this leads to an increase of the binding energy of such spin-polarized states while the polarization increases slightly (see Table II). Therefore the clusters are still stable. Further neighbors now taken into account here give a neglectible contribution to the binding energy. It also turns out that for small U a spin flip is not favorable anymore. Instead merely the polarization is changed slightly and we end up with a spin bag.[18]

D. Spin-polarized cluster of 13 mainly parallel copper spins

Now we want to investigate if the ground state of one additional hole is really the state with one turned spin. To this end we change the initial conditions of the self-consistent approach in the way that we turn four spins. The same formalism as in the previous section can be applied.

It turns out self-consistently that we get a cluster with 13 mainly parallel spins, which is shown in Fig. 5. For the usual parameter region (see Table III) the binding energy of this state is remarkably smaller than for that calculated in the previous section. Therefore the ground state for one additional hole is built up by the smaller cluster.

Increasing U makes larger clusters energetically favorable. This is in agreement with the Nagaoka theorem[19] which states for infinite U an additional hole leads to a ferromagnetic ground state.

In the case of four turned spins the energy-level split off from the upper oxygen band into the charge-transfer gap is separated into four sublevels. Thus we now have the opportunity to remove more than one electron.

As one can see from Table III the binding energy for the case of two or three holes certainly increases but does not reach two or three times the value of the binding energies calculated in Sec. II C. For that reasons two or three additional holes would create two or three separated small clusters.

In Table III one can clearly observe the decrease of the polarization with increasing the number of holes N. With increasing N, $\langle n_\downarrow^{d'} \rangle^n$ becomes smaller while $\langle n_\uparrow^{d'} \rangle^n$ increases. Even if an unpolarized state cannot be calculated in such a mean-field calculation, we can interpret this as a first step towards metallization in a higher-doped percolative network of such clusters.

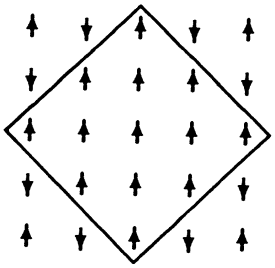

FIG. 5. In this calculation five copper sites were regarded self-consistently but four copper spins were turned.

TABLE II. In this situation five copper sites were regarded self-consistently and the copper spin on the central site was turned. The occupation numbers of the central site $\langle n_\uparrow^{d'} \rangle^c, \langle n_\downarrow^{d'} \rangle^c$, of the four next neighbors $\langle n_\uparrow^{d'} \rangle^n, \langle n_\downarrow^{d'} \rangle^n$ and the binding energy $-\Delta E/T$ are listed.

U	ϵ	N	$\langle n_\uparrow^d \rangle$	$\langle n_\downarrow^d \rangle$	$\langle n_\uparrow^{d'} \rangle^c$	$\langle n_\downarrow^{d'} \rangle^c$	$\langle n_\uparrow^{d'} \rangle^n$	$\langle n_\downarrow^{d'} \rangle^n$	$-\Delta E$
8	5	1	0.217	0.996	0.85	0.28	0.98	0.22	0.34
8	3	1	0.116	0.998	0.80	0.16	0.96	0.14	0.43

III. INFLUENCE OF U_p AND U_{pd} ON POLARIZATION AND BINDING ENERGY

In this section we want to examine how the Coulomb repulsion U_p on oxygen sites and the intersite Coulomb repulsion U_{pd} between electrons on neighboring copper and oxygen atoms affect stability and polarization of spin-polarized clusters. These two additional interactions are taken into account by adding to (1) the Hamiltonians

$$H_{\mathrm{int}}^p = U_p \sum_{m'} n_{m'\uparrow}^p n_{m'\downarrow}^p \tag{30}$$

and

$$H_{\mathrm{int}}^{pd} = U_{pd} \sum_{\substack{(mm') \\ \sigma\sigma'}} n_{m\sigma}^d n_{m'\sigma'}^p \tag{31}$$

(30) and (31) are again treated in the mean-field approximation, yielding

$$H_{\mathrm{int}}^p \approx U_p \sum_{m'\sigma} \langle n_{m'-\sigma}^p \rangle n_{m'\sigma}^p - U_p \sum_{m'} \langle n_{m'\uparrow}^p \rangle \langle n_{m'\downarrow}^p \rangle \ , \tag{32}$$

$$\begin{aligned} H_{\mathrm{int}}^{pd} \approx U_{pd} \sum_{\substack{(mm') \\ \sigma}} & [(\langle n_{m'\sigma}^p \rangle + \langle n_{m'-\sigma}^p \rangle) n_{m\sigma}^d \\ & + (\langle n_{m\sigma}^d \rangle + \langle n_{m-\sigma}^d \rangle) n_{m'\sigma}^p] \\ & - U_{pd} \sum_{\substack{(mm') \\ \sigma\sigma'}} \langle n_{m\sigma}^d \rangle \langle n_{m'\sigma'}^p \rangle \ . \end{aligned} \tag{33}$$

TABLE III. A cluster of 13 mainly parallel copper spins is formed. The binding energy $-\Delta E/T$ is calculated for different numbers of holes (N) inside the cluster.

U	ϵ	N	$\langle n_\uparrow^d \rangle$	$\langle n_\downarrow^d \rangle$	$\langle n_\uparrow^{d'} \rangle^c$	$\langle n_\downarrow^{d'} \rangle^c$	$\langle n_\uparrow^{d'} \rangle^n$	$\langle n_\downarrow^{d'} \rangle^n$	$-\Delta E$
8	3	1	0.217	0.996	0.22	0.94	0.20	0.97	−0.14
8	3	2	0.217	0.996	0.21	0.95	0.29	0.93	0.14
8	3	3	0.217	0.996	0.21	0.95	0.30	0.88	0.45
8	5	1	0.116	0.998	0.13	0.92	0.12	0.96	0.25
8	5	2	0.116	0.998	0.13	0.92	0.13	0.91	0.61
8	5	3	0.116	0.998	0.12	0.92	0.14	0.86	0.96

This leads to a renormalization of the on-site energies. We add the operator-dependent first parts of (32) and (33) to H_{MF}^{σ} (4) and proceed in the same way as in Sec. II A, i.e., we again consider a fixed spin direction and then transform the Hamiltonian into k space. Then we obtain the same Hamilton matrix as (7), but now with differently renormalized parameters

$$\begin{aligned}\epsilon_{1,2}&=\epsilon_d+U\langle n^d_{\downarrow,\uparrow}\rangle+2U_{pd}\langle N^p_{\uparrow}\rangle\ ,\\ \epsilon_p\rightarrow\tilde{\epsilon}_p&=\epsilon_p+2U_{pd}(\langle n^d_{\uparrow}\rangle+\langle n^d_{\downarrow}\rangle)+\frac{U_p}{4}\langle N^p_{\uparrow}\rangle\ ,\end{aligned}\tag{34}$$

where

$$N^p_{\sigma}=\sum_{(m')}n^p_{m'\sigma}\ .\tag{35}$$

The parentheses around m' mean that the summation extends over the four oxygen sites m' neighboring to the copper site m. Due to translational symmetry N^p_{σ} does not depend on m. C_{4v} symmetry implies $\langle n^p_{m'\sigma}\rangle=\langle N^p_{\sigma}\rangle/4$. Further we supposed $\langle N^p_{\uparrow}\rangle=\langle N^p_{\downarrow}\rangle$, which is valid in the undoped case. The spin densities have to be determined self-consistently via the imaginary parts of the Green's functions, which have the same form as in Sec. II A, but with differently renormalized parameters.

A. Self-consistent variation at one copper site

As in Sec. II B, we introduce a local perturbation to the system in the doped case, i.e., we allow the copper spin at site $m=0$ to change its original direction. The expectation values at this site therefore change from $\langle n^d_{\sigma}\rangle$ to $\langle n^{d'}_{\sigma}\rangle$. Due to the intersite Coulomb interaction U_{pd} this leads also to new on-site energies at the four surrounding oxygen sites. Therefore we obtain the following perturbation matrix:

$$\mathbf{V}^{\sigma}=\begin{bmatrix}a_{-\sigma}&0&0&0&0\\0&b&0&0&0\\0&0&b&0&0\\0&0&0&b&0\\0&0&0&0&b\end{bmatrix}\ ,\tag{36}$$

where

$$\begin{aligned}a_{-\sigma}&=U(\langle n^{d'}_{-\sigma}\rangle-\langle n^d_{-\sigma}\rangle)\ ,\\ b&=U_{pd}\sum_{\sigma}(\langle n^{d'}_{\sigma}\rangle-\langle n^d_{\sigma}\rangle)\ ,\end{aligned}\tag{37}$$

and the chosen basis system is

$$|1\rangle=d^{\dagger}_{0\sigma}|0\rangle\quad |i\rangle=p^{\dagger}_{i\sigma}|0\rangle\quad (i=2,\ldots,5)\ .\tag{38}$$

(The four surrounding oxygen sites are labeled by the numbers 2, . . . , 5.)

As the perturbation matrix has the same form as in Sec. II C, we can also apply the transformation **T** in order to solve the Dyson equation for the Green's function **G**. The disturbed spin densities at the site $m=0$ are then determined by the equation

$$\langle n^{d'}_{\sigma}\rangle=\frac{1}{\pi}\int_{-\infty}^{E_F}\mathrm{Im}G^{\sigma}_{11}(E)dE\ .\tag{39}$$

As in Sec. II C we have to deal with localized states which are determined by the equation

$$\det(1-\mathbf{G}^{0\sigma}\mathbf{V}^{\sigma})=0\ .\tag{40}$$

The energy change due to the perturbation is again given by

$$\Delta E=\Delta E^{\mathrm{loc}}+\Delta E^{\mathrm{int}}\ ,\tag{41}$$

where ΔE^{loc} is calculated in the same way as in (21) and ΔE^{int} now reads

$$\begin{aligned}\Delta E^{\mathrm{int}}=&\,U(\langle n^d_{\uparrow}\rangle\langle n^d_{\downarrow}\rangle-\langle n^{d'}_{\uparrow}\rangle\langle n^{d'}_{\downarrow}\rangle)\\ &+U_{pd}\sum_{\sigma\sigma'}(\langle n^d_{\sigma}\rangle-\langle n^{d'}_{\sigma}\rangle)\langle N^p_{\sigma'}\rangle\ .\end{aligned}\tag{42}$$

In Tables IV and V the dependence of the disturbed spin densities in these spin-polarized clusters on U_p and U_{pd} is shown for two sets of parameters U and $\epsilon\equiv\epsilon_p-\epsilon_d$. Tables VI and VII display the binding energy $-\Delta E$.

We observe that the disturbed spin densities $\langle n^{d'}_{\uparrow}\rangle$ and $\langle n^{d'}_{\downarrow}\rangle$ decrease with U_{pd} and increase with U_p. This behavior can easily be understood. The Coulomb repulsion U_{pd} between electrons on neighboring copper and oxygen sites tends to localize the electrons onto the oxygen in order to minimize the corresponding Coulomb energy. This means that the electrons have a higher probability to be on oxygen.

The binding energy of the cluster shows a remarkable behavior. For fixed U_p it first rises with increasing U_{pd} to reach a maximum and then again decreases. For small fixed U_{pd} the magnetic polarons are destabilized by U_p, whereas for larger values of U_{pd} the binding energy $-\Delta E$ increases with U_p up to a certain value in order to fall down thereafter. In Sec. III B we show that this behavior

TABLE IV. Spin densities $\langle n^{d'}_{\uparrow}\rangle,\langle n^{d'}_{\downarrow}\rangle$ for $U/T=6$, $\epsilon/T=2$.

	U_{pd}/T											
U_p/T	0		0.2		0.4		0.6		0.8		1	
0	0.71	0.24	0.66	0.18	0.61	0.14	0.57	0.10	0.54	0.08	0.52	0.06
0.5	0.73	0.28	0.69	0.21	0.64	0.15	0.59	0.12	0.55	0.09	0.53	0.06
1	0.74	0.32	0.71	0.23	0.66	0.17	0.61	0.13	0.57	0.10	0.54	0.07
1.5	0.75	0.36	0.73	0.26	0.69	0.19	0.64	0.14	0.59	0.11	0.56	0.08
2	0.75	0.42	0.74	0.30	0.71	0.22	0.66	0.16	0.61	0.12	0.57	0.09

TABLE V. Spin densities $\langle n_{\uparrow}^{d'} \rangle, \langle n_{\downarrow}^{d'} \rangle$ for $U/T=8$, $\epsilon/T=3$.

	U_{pd}/T											
U_p/T	0		0.2		0.4		0.6		0.8		1	
0	0.79	0.17	0.74	0.14	0.67	0.11	0.60	0.09	0.55	0.07	0.51	0.06
0.5	0.81	0.19	0.77	0.15	0.71	0.12	0.64	0.10	0.57	0.08	0.53	0.06
1	0.82	0.22	0.79	0.16	0.74	0.13	0.67	0.11	0.60	0.09	0.55	0.07
1.5	0.83	0.25	0.81	0.18	0.76	0.14	0.70	0.11	0.63	0.09	0.57	0.08
2	0.84	0.28	0.82	0.21	0.79	0.16	0.73	0.12	0.66	0.10	0.60	0.08

can be understood by considering a simple model of the spin-polarized cluster.

B. Interpretation of the results for the binding energy

1. *Calculation of the delocalization energy in a Mott-Hubbard picture*

In the Mott-Hubbard insulator model double occupancy of copper sites is excluded. This approximation becomes exact for $U \rightarrow \infty$. In this picture the stability of clusters rests on the fact that the kinetic energy of the additional hole strongly depends on the spin orientation of the nearest Cu ions. When the surrounding of the hole is ferromagnetic the hole can delocalize, which leads to a remarkable lowering of the kinetic energy of the system. This gain in kinetic energy is larger than the expense of magnetic energy which is needed for turning the copper spin.[9]

First we want to calculate this delocalization energy. For that purpose we consider the spin-polarized cluster shown in Fig. 6. (The arrows indicate the spins of the holes.) As we are in the large-U limit we exclude the states with copper sites which are doubly occupied with electrons. The state where the additional hole with spin up is located at site number i is denoted by $|i\rangle (i=1,2,\ldots,21)$. The on-site energies are given by

$$\langle i|H|i\rangle = \begin{cases} 15U_p+62U_{pd}+31\epsilon_p+5\epsilon_d =: A; & i=2,\ldots,5 \vee i=10,\ldots,21 \\ 16U_p+56U_{pd}+32\epsilon_p+4\epsilon_d =: B; & i=1 \vee i=6,\ldots,9 \;. \end{cases} \tag{43}$$

The symmetry group of our system is C_{4v}. The eigenfunction to the lowest-energy eigenvalue is invariant under all symmetry transformations of the group C_{4v}, i.e., it belongs to the irreducible representation A_1 of this group. As we are interested only in the ground-state energy it is sufficient to project the Hamiltonian on the basis functions belonging to A_1, which can be found by using the Wigner formula

$$\begin{aligned} |\Psi_1\rangle &= |1\rangle \;, \\ |\Psi_2\rangle &= \tfrac{1}{2}(|2\rangle+|3\rangle+|4\rangle+|5\rangle) \;, \\ |\Psi_3\rangle &= \tfrac{1}{2}(|6\rangle+|7\rangle+|8\rangle+|9\rangle) \;, \\ |\Psi_4\rangle &= \tfrac{1}{2}(|11\rangle+|14\rangle+|17\rangle+|20\rangle) \;, \\ |\Psi_5\rangle &= \frac{1}{\sqrt{8}}(|10\rangle+|13\rangle+|16\rangle+|19\rangle+|12\rangle \\ &\quad +|15\rangle+|18\rangle+|21\rangle) \;. \end{aligned} \tag{44}$$

In this basis the Hamiltonian (1)+(30)+(31) reads

$$H = \begin{bmatrix} B & 2T & 0 & 0 & 0 \\ 2T & A & T & 0 & 0 \\ 0 & T & B & T & \sqrt{2}T \\ 0 & 0 & T & A & 0 \\ 0 & 0 & \sqrt{2}T & 0 & A \end{bmatrix} . \tag{45}$$

The lowest eigenvalue of this matrix is given by

$$E_0^{\text{Ferro}} = \frac{A+B}{2} - \sqrt{[(A-B)/2]^2+6T^2} \;. \tag{46}$$

In comparison to that we calculate the kinetic energy of a hole in an antiferromagnetic surrounding, which is shown in Fig. 7.

Due to the Pauli principle the hole with spin down cannot move to the Cu sites 6, 7, 8, and 9, i.e., it is confined to a unit consisting of the five central atoms. Our basis thus consists only of five functions. The linear

TABLE VI. Binding energy $-\Delta E$ for $U/T=6$, $\epsilon/T=2$ (in units of T).

	U_{pd}/T					
U_p/T	0	0.2	0.4	0.6	0.8	1
0	0.32	0.35	0.35	0.32	0.29	0.25
0.5	0.28	0.33	0.34	0.33	0.30	0.26
1	0.25	0.30	0.33	0.33	0.30	0.27
1.5	0.21	0.27	0.31	0.32	0.31	0.28
2	0.18	0.24	0.29	0.31	0.31	0.29

TABLE VII. Binding energy $-\Delta E$ for $U/T=8$, $\epsilon/T=3$ (in units of T).

	U_{pd}/T					
U_p/T	0	0.2	0.4	0.6	0.8	1
0	0.33	0.36	0.38	0.36	0.33	0.29
0.5	0.30	0.34	0.36	0.36	0.34	0.30
1	0.27	0.32	0.35	0.36	0.34	0.31
1.5	0.24	0.29	0.33	0.35	0.34	0.32
2	0.21	0.26	0.30	0.33	0.34	0.32

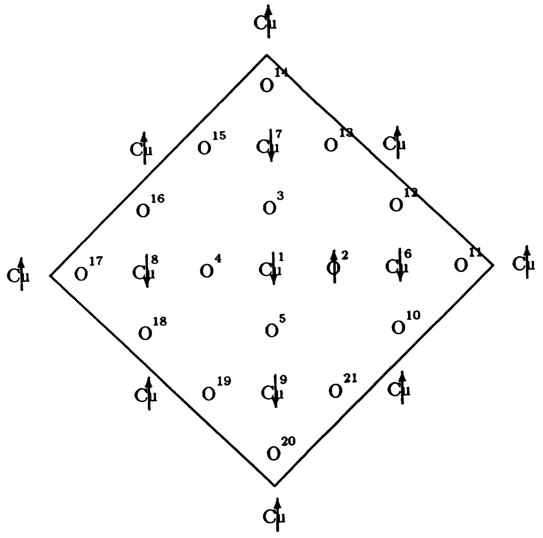

FIG. 6. Additional hole in a ferromagnetic cluster.

combinations belonging to the irreducible representation A_1 are $|\Psi_1\rangle$ and $|\Psi_2\rangle$ which were already given in (44). In this basis the Hamiltonian reads

$$H=\begin{bmatrix} B & 2T \\ 2T & A \end{bmatrix} \tag{47}$$

and its lowest eigenvalue is given by

$$E_0^{\mathrm{AF}}=\frac{A+B}{2}-\sqrt{[(A-B)/2]^2+4T^2}\ . \tag{48}$$

With

$$\begin{aligned} B-A&=U_p-6U_{pd}+\epsilon\ ,\\ \epsilon&=\epsilon_p-\epsilon_d\ . \end{aligned} \tag{49}$$

we finally obtain for the gain of kinetic energy by formation of a spin-polarized cluster

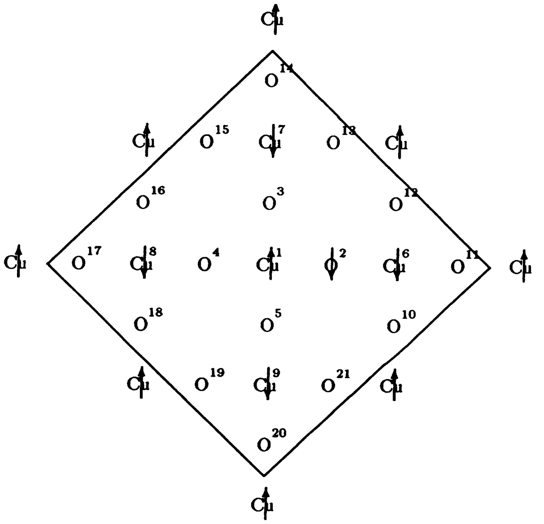

FIG. 7. Additional hole in an antiferromagnetic surrounding.

$$\begin{aligned} -\Delta E^{\mathrm{kin}}&=E_0^{\mathrm{AF}}-E_0^{\mathrm{Ferro}}\\ &=\left[\left[\frac{U_p-6U_{pd}+\epsilon}{2}\right]^2+6T^2\right]^{1/2}\\ &\quad-\left[\left[\frac{U_p-6U_{pd}+\epsilon}{2}\right]^2+4T^2\right]^{1/2} \end{aligned} \tag{50}$$

2. Calculation of the magnetic energy

In this section we want to calculate the influence of U_p and U_{pd} on the expense of magnetic energy necessary for turning one copper spin. To this end we follow a derivation of the superexchange coupling by Nolting[20] within a semiclassical model. For simplicity we consider a linear antiferromagnetic chain of copper and oxygen ions. A part of this chain is shown in Fig. 8.

The magnetic Cu^{2+} ions are assumed to carry classical spins $\mathbf{S}_1,\mathbf{S}_2$ of constant length, but variable orientation. $\mathbf{S}_1$ and $\mathbf{S}_2$ shall enclose the angle θ.

The following configurations are allowed:

(1) Both p electrons are located at the oxygen site. This state has the energy $E_1:=2\epsilon_p+2\epsilon_d+U_p+8U_{pd}$.

(2) The p electron with spin down is found at Cu in 1. The energy is $E_2:=\epsilon_p+3\epsilon_d+U+9U_{pd}$.

(3) The p electron with spin up is found at Cu ion 2 (also E_2).

(4) Both p electrons are located at the Cu ions. The energy of that state is $E_4:=4\epsilon_d+2U+8U_{pd}$.

In analogy with Ref. 20 we thus obtain the Hamilton matrix

$$H=\begin{bmatrix} E_1 & T & T & 0 \\ T & E_2 & 0 & T\sin\frac{\theta}{2} \\ T & 0 & E_2 & T\sin\frac{\theta}{2} \\ 0 & T\sin\frac{\theta}{2} & T\sin\frac{\theta}{2} & E_4 \end{bmatrix}\ . \tag{51}$$

This Hamiltonian has the ground-state energy (up to fifth order in T)

$$E_0=E_0^{(0)}-J\mathbf{S}_1\cdot\mathbf{S}_2\ , \tag{52}$$

where $E_0^{(0)}$ is an insignificant constant and

$$\begin{aligned} J&=-\frac{2T^4}{S^2(U-\epsilon-U_p+U_{pd})^2(2U-2\epsilon-U_p)}\ ,\\ S&=|\mathbf{S}_i|\quad(i=1,2)\ . \end{aligned} \tag{53}$$

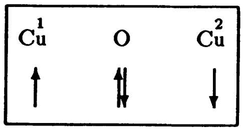

FIG. 8. Linear antiferromagnetic chain of copper and oxygen ions.

The amount of magnetic energy necessary for turning one copper spin is thus

$$\Delta E^{\text{magn}} = -2S^2 J = \frac{4T^4}{(U-\epsilon-U_p+U_{pd})^2(2U-2\epsilon-U_p)} . \tag{54}$$

3. *Binding energy of the cluster*

The binding energy of the spin-polarized cluster is given by

$$\begin{aligned} -\Delta E^{\text{tot}} &= -\Delta E^{\text{magn}} - \Delta E^{\text{kin}} \\ &= -\frac{4T^4}{(U-\epsilon-U_p+U_{pd})^2(2U-2\epsilon-U_p)} \\ &\quad + \left[\left[\frac{U_p-6U_{pd}+\epsilon}{2} \right]^2 + 6T^2 \right]^{1/2} \\ &\quad - \left[\left[\frac{U_p-6U_{pd}+\epsilon}{2} \right]^2 + 4T^2 \right]^{1/2} . \end{aligned} \tag{55}$$

Since we are only interested in a qualitative interpretation of our mean-field results, it is justified to take the ΔE^{magn} calculated for a linear chain, especially as there is no qualitative difference to the two-dimensional case.

The gain of kinetic energy becomes maximal for

$$U_p - 6U_{pd} - \epsilon = 0 , \tag{56}$$

i.e., the maxima of $-\Delta E^{\text{kin}}$ lie on a straight line in a (U_{pd}, U_p) diagram. From $U_p \geq 0$ it follows that $U_{pd} \geq \epsilon/6$, that means that for $U_{pd} < \epsilon/6$ the delocalization energy always decreases with increasing U_p, whereas for $U_{pd} \geq \epsilon/6$ there is a maximum at a certain value of U_p, namely at $U_p = 6U_{pd} - \epsilon$. This is indeed exactly what we observe at the results of our mean-field calculations (see Sec. III A). Further we notice in Tables VI and VII that the maximum of the binding energy of the magnetic polarons in this straight line becomes smaller with increasing U_p or U_{pd}. This is due to the behavior of the magnetic energy. Setting $U_p = 6U_{pd} - \epsilon$ in ΔE^{magn} we get

$$\Delta E^{\text{magn}}\big|_{U_p = 6U_{pd} - \epsilon} = \frac{4T^4}{(U-5U_{pd})^2(2U-\epsilon-6U_{pd})} , \tag{57}$$

which becomes larger with increasing U_{pd}. Summing up, it can be said that the simple model of a spin-polarized cluster presented in this section is able to give a physical insight into the behavior of the binding energy resulting from our mean-field calculations.

IV. INTERACTION BETWEEN NEIGHBORING CLUSTERS

To answer the question if a second hole will go into the same cluster in which a first hole is already situated by simply increasing the size of the magnetic polaron, or if a second hole will create an own cluster we focus on a chain of four and five copper places in the (1,1) direction. Along this chain we variate the occupation numbers of the copper places self-consistently.

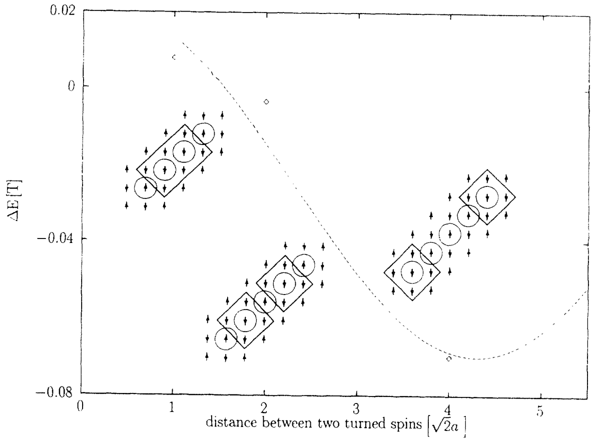

FIG. 9. Two copper spins along a line in the (1,1) direction were turned. For different distances given in units of the lattice constant a, the energy difference for two clusters with infinite distance (zero-line) is plotted. The situation around the two additional holes is shown in the small pictures inside. This was done for a Hubbard repulsion $U/T=8$ and $\epsilon/T=3$. (The dashed line is a guide to the eye.)

The energies of two turned spins at different places on this chain are calculated (see Fig. 9). ΔE is the difference between the binding energy of two turned spins in the chain and the energy of two turned spins with infinite distance.

Although we have only calculated three different distances we can clearly see an influence of the interaction between two clusters. This interaction leads to an attraction of clusters relatively far away from each other. The energy of the interaction has a minimum of approximately 5–9 lattice constants. It gives a slightly repulsive contribution for two turned spins directly beside each other forming a single cluster of eight parallel copper spins. In any case the attraction between two clusters in two dimensions is extremely small compared with the binding energy.

V. CONCLUSION

We have shown that the ground state of a CuO_2 layer with a single defect electron (hole) described by the three band Hubbard model is formed by a spin-polarized cluster (magnetic polaron) with 5–8 parallel copper spins. The binding energy of such a magnetic polaron is of the order of 0.4–0.5 eV. This gives a possible interpretation of 0.3–0.5 eV features in the excitation spectra, which are measured in nearly all cuprate superconductors with infrared spectroscopy.[21]

To describe the influence of higher doping we calculated larger clusters (13 parallel copper spins) containing up to three additional holes. The decrease of the cluster polarization with increasing the number of holes indicates the way in which an antiferromagnetic insulator-metal transition is performed at higher doping.

Further on the influence of the Coulomb repulsions U_p

between electrons on oxygen sites and U_{pd} between electrons on neighboring copper and oxygen sites on the formation of magnetic polarons was investigated. We found that on a straight line in a (U_{pd}, U_p) diagram, which is approximately given by $U_p = 6U_{pd} - \epsilon$, the binding energy of spin-polarized clusters is maximal. For small U_{pd} and U_p these maxima can even be larger than the binding energy in the case $U_{pd} = U_p = 0$. However the essential point is that also at higher values of U_p and U_{pd} the clusters are still stable, because the binding energies only change slightly.

It turned out that two clusters slightly attract each other but only up to a certain distance. Therefore in the low-doping region a second hole will not simply increase the size of an already existing cluster but will form a second independent cluster.

ACKNOWLEDGMENT

The authors would like to acknowledge financial support from the Bundesministerium für Forschung und Technologie.

---

[1] E. L. Nagaev, J. Magn. Magn. Mater. **110**, 39 (1992).

[2] A. F. Barabanov, L. A. Maksimov, and G. V. Uĭmin, Sov. Phys. JETP **69**(2), 371 (1989).

[3] P. Prelovšek, Phys. Lett. A **126**(4), 287 (1988).

[4] D. M. Edwards and M. Miyazaki, J. Phys. F **17**, L311 (1987).

[5] J. Inoue and S. Maekawa, Physica B **165&166**, 1029 (1990).

[6] A. Mauger and D. L. Mills, Phys. Rev. B **40**, 4931 (1989).

[7] A. Auerbach and B. E. Larson, Phys. Rev. Lett. **66**, 2262 (1991).

[8] J. Sabczynski, M. Schreiber, and A. Sherman, Phys. Rev. B **48**, 543 (1993).

[9] V. Hizhnyakov and E. Sigmund, Physica C **156**, 655 (1988); V. Hizhnyakov, E. Sigmund, and M. Schneider, Phys. Rev. B **44**, 795 (1991).

[10] G. Wübbeler and O. Schirmer, Phys. Status Solidi B **174**, K21 (1992).

[11] J. Mesot, P. Allenspach, U. Straub, A. Furrer, and H. Mutka, Phys. Rev. Lett. **70**, 865 (1993).

[12] R. K. Kremer, E. Sigmund, V. Hizhnyakov, F. Hentsch, A. Simon, K. A. Müller, and M. Mehring, Z. Phys. B **86**, 319 (1992).

[13] M. Schluter, J. Hybertsen, and N. E. Christensen, Physica C **153**, 1217 (1988).

[14] E. B. Stechel and D. R. Jennison, Phys. Rev. B **38**, 4632 (1988).

[15] G. Seibold, E. Sigmund, and V. Hizhnyakov, Phys. Rev. B **48**, 7537 (1993).

[16] A. M. Oleś and J. Zaanen, Phys. Rev. B **39**, 9175 (1989).

[17] *Proceedings of the ERICE-Workshop on Phase Separation in Cuprate Superconductors,* edited by G. Benedek and K. A. Müller (World Scientific, Singapore, 1992).

[18] J. R. Schrieffer, X. G. Wen, and S. C. Zhang, Phys. Rev. Lett. B **60**, 944 (1988).

[19] Y. Nagaoka, Phys. Rev. B **147**, 392 (1966).

[20] W. Nolting, *Quantentheorie des Magnetismus 1* (Teubner, Stuttgart, 1986).

[21] J. D. Perkins, J. M. Graybeal, M. A. Kastner, R. J. Birgeneau, J. P. Falck, and M. Greven, Physica B **194-196**, 1533 (1994).

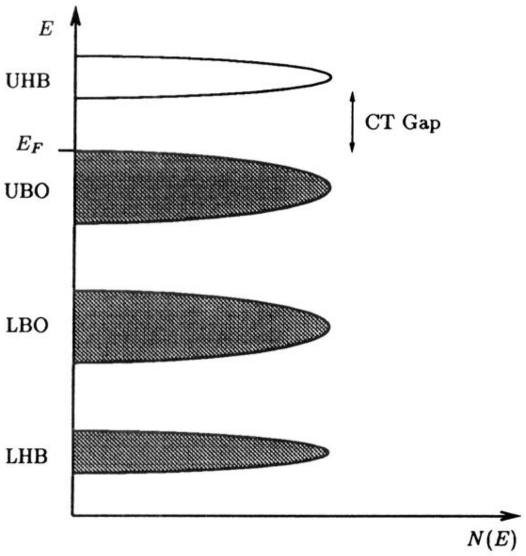

FIG. 1. Bandstructure of the unperturbed antiferromagnet. LHB = lower Hubbard band, UHB = upper Hubbard band, LBO = lower band oxygen, UBO = upper band oxygen.